



CHORUS

This is the accepted manuscript made available via CHORUS. The article has been published as:

Field-Induced Percolation of Polar Nanoregions in Relaxor Ferroelectrics

S. Prosandeev, Dawei Wang, A. R. Akbarzadeh, B. Dkhil, and L. Bellaiche

Phys. Rev. Lett. **110**, 207601 — Published 16 May 2013

DOI: [10.1103/PhysRevLett.110.207601](https://doi.org/10.1103/PhysRevLett.110.207601)

Field-induced Percolation of Polar Nanoregions in Relaxor Ferroelectrics

S. Prosandeev^{1,2}, Dawei Wang³, A. R. Akbarzadeh⁴, B. Dkhil⁵ and L. Bellaiche¹

¹*Physics Department and Institute for Nanoscience and Engineering,
University of Arkansas, Fayetteville, Arkansas 72701, USA*

²*Physics Department and Institute of Physics, South Federal University, Russia*

³*Electronic Materials Research Laboratory,
Key Laboratory of the Ministry of Education
and International Center for Dielectric Research,
Xi'an Jiaotong University, Xi'an 710049, China*

⁴*Wiess School of Natural Sciences, Rice University,
6100 Main Street, MS-103, Houston, TX 77005, USA*

⁵*Laboratoire Structures, Propriétés et Modélisation des Solides,
CNRS-UMR 8580, Ecole Centrale Paris,
Grande Voie des Vignes, 92295 Châtenay-Malabry Cedex, France*

Abstract

A first-principles-based effective Hamiltonian is used to investigate low-temperature properties of Ba(Zr,Ti)O₃ relaxor ferroelectrics under an increasing *dc* electric field. This complex system progressively develops an electric polarization that is highly non-linear with the *dc* field. This development leads to a maximum of the static dielectric response at a critical field, E_{th} , and involves four different field regimes. Each of these regimes is associated with its own characteristic behavior of polar nanoregions (PNRs), such as shrinking, flipping and elongation of dipoles or change in morphology. Strikingly, clusters propagating inside the *whole* sample, with dipoles being parallel to the field direction, begin to form at precisely the E_{th} critical field. Such result, and further analysis we performed, therefore reveal that field-induced percolation of PNRs is the driving mechanism for the transition from the relaxor to ferroelectric state.

Relaxor ferroelectrics exhibit a frequency-dependent and broad dielectric response around some specific finite temperature, while they remain macroscopically paraelectric and cubic down to 0K [1]. These complex materials have been extensively studied (see, e.g., Refs. [1–24] and references therein), and one popular scenario to explain such properties is the formation of polar nanoregions (PNRs). Another striking feature of relaxors is that they acquire a macroscopic polarization when a large enough electric field is applied to them. Despite the fact that the transition from relaxor to ferroelectric state has been a topic of many studies [25–33], several issues related to it are still unknown or controversial. For instance, how PNRs individually and collectively respond to an electric field, in order to render the system ferroelectric, is an open question. Ideally, one would also like to know if there is an universal mechanism driving this transition, and if this mechanism can be described by percolation [34] – which is a fundamental theory that has sometimes been advocated to be responsible for a *temperature*, rather than field, induced transition from relaxor to ferroelectric state [35–38].

The goal of this Letter is to resolve this paucity of knowledge by investigating a Ba(Zr,Ti)O₃ (BZT) system under *dc* electric fields, from first principles. Such compound was chosen because it is a relaxor that has attracted a lot of attention [39–47], and because recent computations successfully showed the existence of static PNRs there at low temperatures [48] (this feature being a key ingredient for understanding relaxor behavior in that system). Our present *ab-initio* simulations reveal that the field-driven transition from a relaxor to ferroelectric state involves four different field regimes in BZT, each associated with their own specific change in morphology of the PNRs or evolution of the dipoles inside these PNRs. Another important finding is that percolation is indeed discovered to be at the heart of this transition. However, in contrast to conventional percolation theory, it is the field’s magnitude that is playing here the role typically assigned to the composition, with the objects percolating being the PNRs’ dipole moments (rather than sites and bonds).

We use the first-principles-based effective Hamiltonian approach that has been recently developed for BZT solid solutions [48]. More details about this approach is provided in the Supplementary Material and involves the quotation of Refs. [48–57]. Here, we apply electric field lying along the [111] pseudo-cubic direction, and having magnitude varying between 0 and 2×10^8 V/m. $12 \times 12 \times 12$ supercells (8640 atoms) are typically used within Monte-Carlo simulations, but larger supercells were also tested to check the convergency of

our results. In all these supercells, Zr and Ti ions are initially randomly distributed over the B-sublattice and then kept frozen, in order to mimic *disordered* BZT solid solutions. Practically, 20 different random configurations are selected and properties to be shown are averaged over all these realizations of disordered systems.

As shown in Ref. [48], this effective Hamiltonian predicted that PNRs – all possessing Ti ions that are displaced along one of the eight $\langle 111 \rangle$ directions – exist within a Zr-rich paraelectric matrix in disordered $\text{Ba}(\text{Zr}_{0.5}\text{Ti}_{0.5})\text{O}_3$ compounds, when no field is applied and for temperatures below $\simeq 130\text{K}$ [58]. This latter critical temperature was identified as the freezing temperature in Ref.[39]. The overall polarization of the whole sample was found to vanish in that case, because different PNRs exhibit Ti displacements along different $\langle 111 \rangle$ directions. Figure 1a provides a snapshot of the dipolar configurations in a (y, z) plane at 10K when no external field is applied. Ti ions belonging to PNRs existing in this plane are identified and delimited by means of red solid lines there. For instance, clusters ‘2’ and ‘5’ have dipoles all nearly aligned along $[111]$, while cluster ‘3’ exhibits a local polarization lying along $[\bar{1}\bar{1}\bar{1}]$ and clusters ‘6’ and ‘7’ possess electric dipoles being along $[1\bar{1}\bar{1}]$ and $[\bar{1}11]$, respectively, in that (y, z) plane. Note that PNRs are practically determined by continuously attempting to add new (first-nearest neighbors) dipoles to a given PNR, and by accepting such dipoles if the condition of a 90% likelihood (as computed by Bayesian methods [59]) of their direction with respect to that of the dipoles already existing inside the PNR is satisfied.

Figure 2 shows the behavior of the overall polarization as a function of an increasing electric field, that is applied along the $[111]$ pseudo-cubic direction. This function is strongly non-linear, which is a known fingerprint of relaxors under electric fields [60] (Note that we also checked (not shown here) that decreasing this field from its maximal investigated value until fully annihilating it results in a small but non-vanishing polarization (of 0.11 C/m^2), which is another known feature of relaxors [60]). As indicated in Fig. 2 by means of solid lines, this polarization-*versus*-field curve can be nicely fitted by the following expression: $P = aE + bE^3 + cE^5 + dE^7$, where P and E are the magnitude of the polarization and electric field, respectively, while a , b , c and d are fitting parameters. The a parameter is directly related to the linear dielectric susceptibility, while b , c and d correspond to *nonlinear* susceptibilities of the order 3, 5 and 7, respectively [61]. We numerically found that a , b , c and d are equal to 61.8×10^{-11} , 18.1×10^{-26} , -86.0×10^{-43} and 17.6×10^{-59} in S.I. units, respectively. Note that c is the only coefficient that is negative in BZT under field

applied along [111], and that we checked that the orders of magnitude and sign of these parameters are unchanged when increasing the supercell size. Taking the derivative of the aforementioned fitting polynomial of order 7 with respect to electric field provides the static dielectric response shown in the inset of Fig. 2. The field behaviors of the polarization and of this dielectric response allow the introduction of four different regions. Region I ranges between 0 and 3×10^7 V/m, and is associated with a nearly linear and slight increase of the polarization when increasing the field – resulting in a relatively small and slightly increasing dielectric response. Then, Region II occurs for fields larger than 3×10^7 V/m but smaller than 1.0×10^8 V/m, and is characterized by a strong deviation from a linear behavior of the polarization with field. Such strong deviation leads to a rapid *increase* of the dielectric constant from $\simeq 100$ to over 300 when the field grows. Region III exists for fields ranging between 10^8 V/m (corresponding to the inflexion point of $P(E)$) and up to 1.7×10^8 V/m, and is also associated with a strong nonlinear dependency of the polarization with field. However, unlike Region II, increasing the field in Region III results in a significant *decrease* of the dielectric constant. Such latter quantity therefore exhibits a maximum at the border between Regions II and III, and the resulting transition from Region II to Region III can be considered as being diffuse (Note that this fact contrasts with the case of $\text{Pb}(\text{Mg},\text{Nb})\text{O}_3$ for which the field-induced relaxor-to-ferroelectric transition can rather be of first order and can be accompanied by a jump in polarization [61]). Finally, for fields larger than 1.7×10^8 V/m, Region IV happens. It possesses a small, nearly linear variation of the polarization with field, yielding a static dielectric response that is quite small and that slightly decreases with the fields’ magnitude.

Let us now focus on Figures 1, in order to gain a microscopic understanding of the polarization-*versus*-field curve of Fig. 2 and of Regions I, II, III and IV. Figures 1 display snapshots of the dipolar configuration in a given (y, z) plane for different magnitude of the applied electric field, E . By comparing Figs. 1a and 1b, one can see that increasing E in Region I does neither affect the morphology of the polar nanoregions that already exist when the field is null nor the direction of their own local polarization. In fact, our simulations reveal that the *magnitude* of the local polarization of these PNRs slightly increases (respectively, decrease) with E if this local polarization lies (respectively, does *not* lie) along the field direction. Such microscopic evolution is mostly responsible for the small change of the overall polarization with field in Region I. Note that additional, small clusters also form

in Region I (see, e.g., top left of Fig. 1b), and also contribute to the small change in polarization. Then, progressively increasing E in Region II has three dramatic consequences: (1) large PNRs with local dipoles that are *not* initially aligned along the field direction considerably shrink in size and have some of their dipoles flipped towards the field’s direction (*cf* the evolution of cluster 3 between Figs. 1b and 1c); (2) Novel large clusters with dipoles lying along the direction of the electric field form (see top left of Fig. 1c); and (3) Ti clusters that initially possessed dipoles being along the field direction grow in size (see the expansion of clusters 2 and 5 when going from Fig. 1b to 1c). Items (1)-(3) are responsible for the strong non-linear behavior of the overall polarization, and the resulting enhancement of the dielectric response, with field in Region II. Increasing E in Region III continues to lead to the shrinking, or even annihilation, of some small clusters if their dipoles are not aligned along the field direction (see the PNR at the bottom right of Fig. 1c that disappears in Fig. 1d). As clearly seen in Fig. 1e, its main effect, however, is the formation of rather large PNRs. Such formation occurs via the “merging” of small clusters into large PNRs, via the flipping of dipoles that were in-between these small clusters, as evidenced by comparing Figs. 1c, 1d and 1e. This merging also results in a non-linear behavior of the overall polarization-*versus*-field, but is accompanied by a decrease (rather than an increase) of the static dielectric response. Finally, in Region IV, comparing Figs. 1e and 1f tells us that small and large PNRs mostly experience an increase of the magnitude of their dipoles (that are all aligned along the field’s direction) when increasing the field’s magnitude. This leads to a small, nearly linear increase of the overall polarization and to a relatively small value of the dielectric response. It is interesting to realize that, in Region IV, the dipoles centered on Zr ions are still small in magnitude, which is consistent with a previously suggested idea that a relaxor has two components: a spherical glassy matrix, that does not respond to an electric field, and polar nano clusters that rearrange themselves when under electric field [37]. Moreover, in Region IV, certain Ti dipoles still do not belong to any PNR. Such Ti dipoles are typically those located within a Zr-rich environment and can be small, as consistent with the first-principles work of Ref. [43].

To further understand properties of BZT under an electric field, we decided to check if our results can be analyzed within the context of percolation theory. Accordingly, two different properties were computed from the outputs of our MC simulations. One quantity

is the average cluster size, and is defined as [34]:

$$\langle s \rangle = \langle N^2 \rangle / \langle N \rangle \quad (1)$$

where N is the number of Ti sites belonging to a PNR, and where “ $\langle \ \rangle$ ” denotes average over all the PNRs belonging to the supercell. The other quantity is the so-called strength of the percolating cluster [34], that is calculated as:

$$P_\infty = N_\infty / N_{Ti} \quad (2)$$

where N_∞ is the number of the distinct Ti sites (of the supercell) belonging to the (infinite) percolating cluster, and where N_{Ti} is the number of Ti ions in the supercell [62]. Technically, a cluster is taken to be infinite or percolating when it is found to spread from one side of the supercell to its opposite side along the [100] (x), [010] (y) or [001] (z) direction.

It is important to recall that in “conventional” percolation, that is in percolation induced by composition, x , the average cluster size diverges at the percolation (compositional) threshold, x_c , following a $1/|x_c - x|^\gamma$ behavior, with the γ coefficient depending on the dimensionality and type of the lattice [34]. On the other hand, in conventional percolation, P_∞ starts to rapidly grow for compositions above x_c , adopting a $(x - x_c)^\beta$ power law with the value of β being also tabulated for different dimensionalities and lattices [34].

Figure 3 shows that, in Regions I and II, P_∞ basically vanishes. On the other hand, the strength of the percolating cluster becomes finite and significantly increases when the field increases in Regions III and IV, that is above the critical value, E_{th} , of 10^8 V/m. Interestingly and as also indicated in Fig. 3, the behavior of P_∞ versus the field can be rather well fitted by a $(E - E_{th})^{\beta_E}$ power law for fields above E_{th} . These findings reveal that percolation of the PNRs does take place in BZT at the beginning of Region III, with the magnitude of the static electric field playing the role of composition in conventional percolation theory. Note that β_E is practically found to vary between 0.6 and 0.7, when going from a $12 \times 12 \times 12$ to $16 \times 16 \times 16$ supercell. The inset of Fig. 3 also shows that $\langle s \rangle$ is nearly constant, around 3, in Region I. This reflects the previous finding that PNRs are typically small and their morphologies are not evolving too much, for small fields (see Figs. 1a and 1b). Then, the average cluster size significantly increases when increasing E in Region II. The behavior of $\langle s \rangle$ -versus- E can be well fitted by $1/|E_{th} - E|^{\gamma_E}$. Such results are once again consistent with standard percolation theory, once assuming that the electric field plays the analogous

role of composition. Our simulations performed on a few different supercell sizes provide a value of γ_E ranging between 1.0 and 1.3, which is consistent with the value assumed in Ref. [36] for a temperature-induced percolation in $\text{Pb}(\text{Mg,Nb})\text{O}_3$ relaxor.

The connection between the formation of the field-induced polarization in relaxors and percolation driven by electric fields is therefore found here to explain and understand properties of BZT relaxors under electric fields [63]. For instance, our present work reveals that the maximum of the dielectric response displayed in the inset of Fig. 2 corresponds to the percolation threshold, that is to the minimum field for which an infinite cluster can percolate inside BZT. We therefore hope that our study not only leads to a better understanding of relaxor ferroelectrics (thanks to microscopic insights), but will also open numerous investigations checking/using percolation theory to analyze properties of these fascinating materials (or other complex systems) [72].

This work is financially supported by the ONR Grants N00014-11-1-0384, N00014-12-1-1034, and N00014-08-1-0915. S.P. and L.B. also acknowledge NSF DMR-1066158, Department of Energy, Office of Basic Energy Sciences, under contract ER-46612, and ARO Grant W911NF-12-1-0085 for discussions with scientists sponsored by these grants. D.W. acknowledges support from the National Natural Science Foundation of China under Grant No. 51272204. Some computations were also made possible thanks to the ONR grant N00014-07-1-0825 (DURIP), a Challenge grant from the Department of Defense, as well as MRI grant 0722625, MRI-R2 grant 0959124, and CI-TRAIN grant 0918970 from NSF. S.P. appreciates Grant 12-08-00887-a of Russian Foundation for Basic Research. The authors thank Drs. Bokov, Kleemann and Maglione for insightful discussions.

-
- [1] L. E. Cross, *Ferroelectrics* **151**, 305 (1994).
 - [2] G. Burns, and F. H. Dacol, *Phys. Rev. B* **28**, 2527 (1983).
 - [3] G. A. Smolensky *et al.*, *Ferroelectrics and Related Materials* (Gordon and Breach, New York, 1981).
 - [4] V. Westphal, W. Kleemann and M. D. Glinchuk, *Phys. Rev. Lett.* **68**, 847 (1992).
 - [5] A. K. Tagantsev and A. E. Glazounov, *Phys. Rev. B* **57**, 18 (1998).
 - [6] R. Pirc, and R. Blinc, *Phys. Rev. B* **60**, 13470 (1999).

- [7] I.-K. Jeong *et al.*, Phys. Rev. Lett. **94**, 147602 (2005).
- [8] Y. Bai, and L. Jin, J. Phys. D: Appl. Phys. **41** 152008 (2008).
- [9] H. Vogel, Phys. Z. **22** 645 (1921).
- [10] G. S. Fulcher, J. Am. Ceram. Soc. **8**, 339 (1925).
- [11] B. Dkhil *et al.*, Phys. Rev. B **80**, 064103 (2009).
- [12] O. Svitelskiy *et al.*, Phys. Rev. B **72**, 172106 (2005).
- [13] S. Tinte, B. P. Burton, E. Cockayne and U. V. Waghmare, Phys. Rev. Lett. **97**, 137601 (2006).
- [14] V. M. Ishchuk, V. N. Baumer and V. L. Sobolev, J. Phys.: Condens. Matter **17** L177 (2005).
- [15] N. Takesue, Y. Fujii, M. Ichihara and H. Chen, Phys. Rev. Lett. **82**, 3709 (1999).
- [16] R. Blinc *et al.*, Phys. Rev. B **63**, 024104 (2000).
- [17] B. E. Vugmeister and H. Rabitz, Phys. Rev. B **57**, 7581 (1998).
- [18] D. Viehland, S. J. Jang, L. E. Cross and M. Wuttig, J. Appl. Phys. **68**, 2916 (1990).
- [19] E. V. Colla, E. Y. Koroleva, N. M. Okuneva and S. B. Vakhrushev, Phys. Rev. Lett. **74**, 1681 (1995).
- [20] I. Grinberg, P. Juhas, P. K. Davies, and A. M. Rappe, Phys. Rev. Lett. **99**, 267603 (2007).
- [21] A. Al-Zein, J. Hlinka, J. Rouquette and B. Hehlen, Phys Rev Lett. **105** 017601 (2010).
- [22] Z. Kutnjak *et al.*, Phys. Rev. B **59** 294 (1999).
- [23] A. Levstik, Z. Kutnjak, C. Filipic and R. Pirc, Phys. Rev. B **57**, 11204 (1998).
- [24] A. A. Bokov and Z.-G. Ye, Journal of Advanced Dielectrics **2** 1241010 (2012).
- [25] Z.-G. Ye and H. Schmid, Ferroelectrics **145**, 83 (1993).
- [26] Z. Kutnjak, B. Vodopivec, and R. Blinc, Phys. Rev. B **77**, 054102 (2008).
- [27] Z. Wu, W. Duan, Z. Liu, and B.-L. Gu, Phys. Rev. B **65**, 174119 (2002).
- [28] B. E. Vugmeister and H. Rabitz, Phys. Rev. B **65**, 024111 (2001).
- [29] B. Dkhil and J. M. Kiat, J. Appl. Phys. **90**, 4676 (2001).
- [30] R. Pirc, Z. Kutnjak, R. Blinc, and Q. M. Zhang, J. Appl. Phys. **110**, 074113 (2011).
- [31] N. Novak, R. Pirc, M. Wencka, and Z. Kutnjak, Phys. Rev. Lett. **109**, 037601 (2012).
- [32] I. P. Raevski, S. A. Prosandeev, A. S. Emelyanov, S. I. Raevskaya, Eugene V. Colla, D. Viehland, W. Kleemann, S. B. Vakhrushev, J-L. Dellis, M. El Marssi, and L. Jastrabik, Phys. Rev. B **72**, 184104 (2005).
- [33] R. Pirc, R. Blinc, and Z. Kutnjak, Phys. Rev. B **65**, 214101 (2002).
- [34] D. Stauffer and A. Aharony, *Introduction to Percolation Theory* (Taylor & Francis, London,

- 1994).
- [35] L.S. Kamzina and N.N. Krainik, *Physics of the Solid State* **42**, 142 (2000).
 - [36] R. Pirc and R. Blinc, *Phys. Rev. B* **76**, 020101 (R) (2007).
 - [37] C.S. Tsu *et al*, *Phys. Rev. B* **75**, 212101 (2007).
 - [38] A. Koreeda *et al*, *Phys. Rev. Lett.* **109**, 197601 (2012).
 - [39] R. Fahri, M. E Marssi, A. Simon and J. A. Ravez, *Eur. Phys. J. B* **9**, 599 (1999).
 - [40] T. Maiti, R. Gu, and A. S. Bhalla, *J. Amer. Ceram. Soc.* **91**, 1769 (2008).
 - [41] R. L. L. Withers and B. Nguyen, *Appl. Phys. Lett.* **91**, 152907 (2007).
 - [42] A. Simon, J. Ravez and M. Maglione, *J.Phys.: Condens Matter* **16**, 963 (2004).
 - [43] C. Laulhé, A. Pasturel, F. Hippert and J. Kreisel, *Phys. Rev. B* **82**, 132102 (2010).
 - [44] A. Dixit, S. B. Majumder, R. S. Katiyar and A. S. Bhalla, *J. Mat. Sci.* **41**, 87 (2006).
 - [45] A. A. Bokov, M. Maglione, and Z.-G. Ye, *J. Phys.: Condens. Matter* **19**, 092001 (2007).
 - [46] V.V. Shvartsman, J. Zhai and W. Kleemann, *Ferroelectrics* **379**, 77 (2009).
 - [47] D. Nuzhnyy *et al*, *Phys. Rev. B* **86**, 014106 (2012).
 - [48] A.R Akbarzadeh, S. Prosandeev, E.J. Walter, A. Al-Barakaty and L. Bellaiche, *Phys. Rev. Lett.* **108**, 257601 (2012).
 - [49] W. Zhong, D. Vanderbilt and K. M. Rabe, *Phys. Rev. B* **52**, 6301 (1995).
 - [50] L. Bellaiche, A. García and D. Vanderbilt, *Phys. Rev. Lett.* **84**, 5427 (2000); *Ferroelectrics* **266**, 41 (2002).
 - [51] L. Bellaiche and D. Vanderbilt, *Phys. Rev. B* **61**, 7877 (2000).
 - [52] A.R. Akbarzadeh, I. Kornev, C. Malibert, L. Bellaiche and J.M. Kiat, *Phys. Rev. B* **72**, 205104 (2005).
 - [53] P. Hohenberg and W. Kohn, *Phys. Rev.* **136**, B864(1964).
 - [54] D. Vanderbilt, *Phys. Rev. B* **41**, 7892 (1990).
 - [55] B.-K. Lai, I. Ponomareva, I. I. Naumov, I. A. Kornev, H. Fu, L. Bellaiche and G. J. Salamo, *Phys. Rev. Lett.*, **96**, 137602 (2006).
 - [56] S. Prosandeev, I. Ponomareva, I. Kornev, I. Naumov and L. Bellaiche, *Phys. Rev. Lett.* **96**, 237601 (2006).
 - [57] L. Bellaiche, A. Garcia and D. Vanderbilt, *Phys. Rev. B* **64**, 060103(R) (2001).
 - [58] As found in Ref. [48] by switching on and off parameters of the used effective Hamiltonian, the formation of PNRs originates from (1) the desire of Ti ions to move off center while Zr

- ions energetically prefer to stay at ideal cubic sites, and (2) antiferroelectric-like interactions between different Ti-rich clusters. Random fields and random strains are found to be negligible to understand the relaxor behavior of the isovalent BZT system, as consistent with Ref. [45].
- [59] E. T. Jaynes , *Probability Theory: The Logic of Science* (Cambridge University Press, 2003).
- [60] G. A Samara, J. Phys.: Condens. Matter **15**, 367 (2003).
- [61] R. Pirc, Z. Kutnjak, and N. Novak, J. Appl. Phys. **112**, 114122 (2012); arXiv:1210.6530v1 (2012).
- [62] Note that $\langle s \rangle$ and P_∞ are also averaged over the 20 different supercells chosen to mimic disordered BZT solid solutions.
- [63] It is worthwhile to realize that Refs. [64, 65] also use the concept of a percolation that is induced by a quantity that is *not* the sole composition (namely, the temperature there) to explain different phenomena. Moreover, the use of the field as a parameter driving critical phenomena in disordered systems has also been considered in Refs. [66, 67]. It may also be interesting to develop novel theories for inhomogenous materials, based on domain growth [68–70] or filament formation [71], to analyze (in a different way) the present numerical data.
- [64] L. Gor’kov and V. Kresin, Journal of Superconductivity **13**, 239 (2000).
- [65] V.A. Trepakov *et al*, Journal of Physics and Chemistry of Solids **65**, 1317(2004).
- [66] T. Nattermann, V. Pokrovskiy, and V.M. Vinokur, Phys. Rev. Lett. **87**, 197005 (2001).
- [67] K. Binder and A. P. Young, Rev Mod Phys **58**, 801 (1986).
- [68] Y. Ishibashi and Y. Takagi, J. Phys. Soc. Jpn. **31**, 506 (1971).
- [69] M. Avrami, J. Chem. Phys. **7**, 1103 (1939).
- [70] A. N. Kolmogorov, Izv. Akad. Nauk USSR, Ser. Math. **3**, 355 (1937).
- [71] Y.C. Yang and W. Lu, Nature Communications **3**, 732 (2012).
- [72] For instance, it is interesting to realize that our results are somehow consistent with the previous X-ray diffraction measurements performed on a single crystal of $\text{Pb}(\text{Mg,Nb})\text{O}_3$ (PMN) relaxor, that is preliminarily cooled down below the freezing temperature and then subjected to a fixed electric field being larger than the threshold one [73]. However, such consistency occurs once substituting the electric field’s magnitude of our computations by the time elapsed since the field has been applied in the measurements. As a matter of fact, in that experimental study [73], it was shown that: (i) before a threshold time, the macroscopic polarisation first weakly and linearly increases with time, while the cluster size remains unchanged (which

corresponds to our Region I); then (ii) the polarization significantly accelerates with time (Region II in our model); and (iii) finally, at a threshold time, a ferroelectric state is achieved by coalescence of polar clusters through their percolation (Region III in our case). This observed time dependence (at fixed electric field) of the field-induced ferroelectric state in PMN relaxor is therefore rather similar to our predicted field dependence of the field-induced ferroelectric state in BZT relaxor. Note, however, that PMN is different from BZT, in the sense that random fields and skin effects [74, 75] can be important to explain relaxor behavior in the former material.

[73] S. Vakhrushev *et al.*, Solid State Com. **103**, 477 (1997).

[74] C. Stock *et al.*, Phys. Rev. B **76**, 064122 (2007).

[75] R.A. Cowley *et al.*, Advances in Physics **60**, 229 (2011).

FIGURE CAPTIONS

Figure 1: (color online) Snapshots of the dipolar configurations in a given (y, z) plane for different magnitude of an electric field applied along the [111] direction in disordered $\text{Ba}(\text{Zr}_{0.5}\text{Ti}_{0.5})\text{O}_3$ solid solutions, at 10K. Panels (a), (b), (c), (d), (e) and (f) correspond to field's magnitude of 0 V/m (Region I), 3×10^7 V/m (Regions I/II), 8×10^7 V/m (Region II), 1.2×10^8 V/m (Region III), 1.7×10^8 V/m (Regions III/IV), and 2.0×10^8 V/m (Region IV), respectively. Green color indicates that the corresponding local modes are centered on Zr ions. Blue and black colors indicate that the corresponding local modes are centered on Ti ions, and that the corresponding x -component of these local modes are negative and positive, respectively. Red color is used to delimit PNRs. The clusters appearing in Panel (a) are denoted by numbers varying between 1 and 8.

Figure 2: (color online) Dependency of the overall macroscopic polarization on the magnitude of the electric field applied along the [111] direction in disordered $\text{Ba}(\text{Zr}_{0.5}\text{Ti}_{0.5})\text{O}_3$ solid solutions, at 10K. The red line represents a fitting of the numerical data by a specific polynomial (see text). The inset displays the static dielectric response that can be derived from that polynomial. The range of occurrence of Regions I, II, III and IV (see text) are indicated via the use of vertical dashed lines.

Figure 3: (color online) Dependency of the strength of the percolating cluster on the magnitude of the electric field applied along the [111] direction in disordered $\text{Ba}(\text{Zr}_{0.5}\text{Ti}_{0.5})\text{O}_3$ solid solutions, at 10K. The red line is a guide for the eyes for fields below E_{th} , while it represents the power law discussed in the text for fields above that critical value. The inset shows the average size cluster as a function of field, when this latter is smaller than E_{th} . The red line in this inset is a fit by a function that is also indicated and discussed in the text. The range of occurrence of Regions I, II, III and IV are indicated via the use of vertical dashed lines.

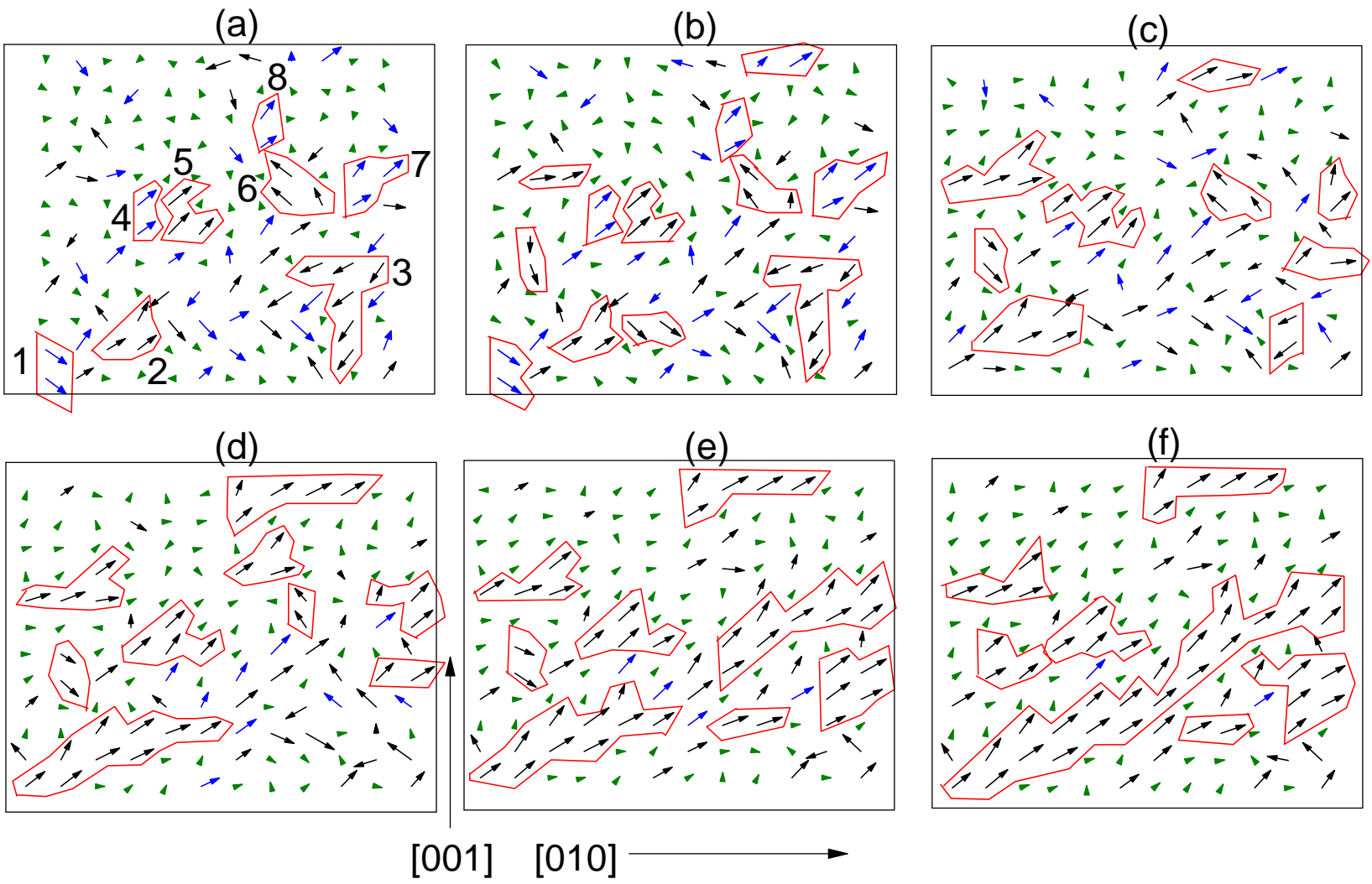


Figure 1 LZ12858 10Apr2013

Figure 2 LZ12858 10Apr2013

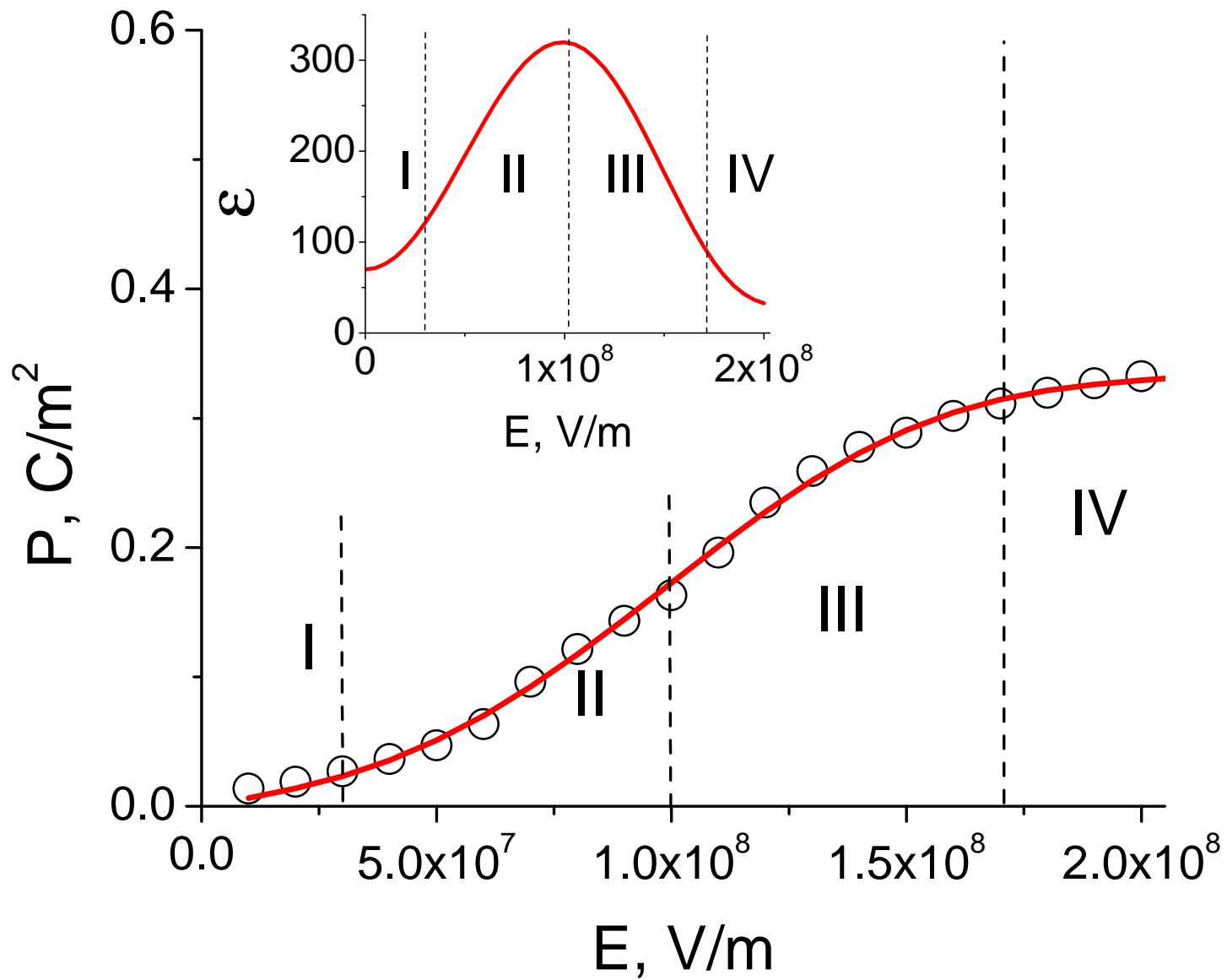


Figure 3 LZ12858 10Apr2013

